



Adsorptive removal of copper (II) ions from aqueous solution by silane cross-linked chitosan/PVA/TEOS beads: kinetics and isotherms

Muhammad Arif Kamal^{a,b}, Tariq Yasin^a, Laurence Reinert^{b,*}, Laurent Duclaux^b

^aDepartment of Metallurgy & Materials Engineering, Pakistan Institute of Engineering & Applied Sciences, Islamabad, Pakistan, Tel. +92 51 9248610; Fax: +92 51 2208070; email: arifkamal14@yahoo.com (M.A. Kamal), yasintariq@yahoo.com (T. Yasin)

^bUniv. Savoie Mont Blanc, LCME, 73000 Chambéry, France, Tel. +33(0)479758122; Fax: +33(0)479758674; email: laurence.reinert@univ-savoie.fr (L. Reinert), Tel. +33(0)479758805; Fax: +33(0)479758674; email: laurent.duclaux@univ-savoie.fr (L. Duclaux)

Received 11 July 2014; Accepted 17 November 2014

ABSTRACT

In this study, beads of chitosan (CS) containing polyvinyl alcohol (PVA) were prepared and cross-linked with tetraethoxysilane (TEOS). The cross-linking of CS/PVA beads with TEOS preserved the active adsorption sites of CS and also enhanced its chemical and mechanical stability. The chemical solubility test and swelling behavior of the beads were studied, especially, in acidic media. Adsorbents were characterized by infrared spectroscopy and scanning electron microscopy. The removal of Cu²⁺ ions from aqueous solution on the prepared beads was investigated in a batch adsorption system as a function of pH, amount of adsorbent, initial concentration of metal ions, and contact time. The adsorption data were analyzed on the basis of Lagergren pseudo-first-order, pseudo-second-order and interparticle diffusion models. Experimental data were fitted with Langmuir and Freundlich isotherm models. The maximum adsorption capacity of cross-linked CS/PVA/TEOS beads for copper ions was of 224.6 mg/g according to Langmuir isotherm for Cu²⁺ ions. The calculated thermodynamic parameters (ΔG° , ΔH° and ΔS°) indicated a spontaneous and endothermic adsorption reaction.

Keywords: Adsorption; Copper; Chitosan; Composite; Beads; PVA

1. Introduction

In the past few decades, the environmental contamination of heavy metals has arisen as a special concern because of their high toxicity and nonbiodegradability [1]. In connection to global industrial activities, the production and consumption of heavy metals have been increased tremendously, which caused to increase discharge of metal ions into the environment (for example Pb, Ni, Cu, Cr, Mn, Hg, Zn, and Cd).

Contamination of heavy metals in water reserves is also a worrying issue to all living organisms, including human beings, animals and plants [2,3]. Unlike organic pollutants, the most of which are vulnerable to biological degradation, heavy metals are not converted into nontoxic end products. So, the removal of these heavy metal ions from water and wastewater is vital to protect our environment [4]. In the animal's metabolism, copper has a key role because it is a major component of various enzymes responsible for catalytically redox reactions. But its disorder may

*Corresponding author.

cause vomiting, cramps, convulsions, or even death in case of excessive incorporation of copper [5].

Many techniques, such as ion exchange, precipitation, reverse osmosis, coagulation, membrane separation, electrolysis, evaporation, etc. are being employed to remove heavy metal ions from industrial wastes. These techniques are mostly expensive and unprofitable, especially, for solution having low concentration of metals. Among the conventional techniques, adsorption process is particularly selected when the upgrading of trace metal quantities or the selectivity of some particular metal is required [6,7]. Nowadays, researchers have keen interest to produce common, low cost, naturally available, and renewable adsorbent alternatives to synthetic polymer for the removal of heavy metal ions [8–11]. Such a polymer is chitosan (CS), which is formed of randomly distributed β -[1 \rightarrow 4]-linked D-glucosamine (de-acetylated unit) and N-acetyl-D-glucosamine units, and is produced by the deacetylation (DDA) of polysaccharide chitin extracted from crustacean shells with NaOH [12,13]. CS is widely used due to its biodegradability, biocompatibility, hydrophilicity, harmless to the living things and ease of chemical derivatization. Moreover, a lot of amino and hydroxyl groups present in CS allow the uptake of heavy metal ions by following different mechanisms, such as chelation, electrostatic attraction or ion-exchange, depending on the metal ion and the pH of the solution. Adsorption capacity of CS is mainly dependent of its amino group, crystallinity, and affinity toward water and degree of DDA. On the other hand, a major drawback of CS is that it instantly dissolves in acidic condition. Chemical modifications were proposed to improve the mechanical strength and the chemical stability of the CS in acidic media [14–16]. Cross-linking of polymers is one form of chemical modification. Various cross-linking agents e.g. glutaraldehyde, epichlorohydrin, ethylene glycol diglycidyl ether, etc. were used to make CS stable in acid solutions. This process had adverse influence on its loading capacity due to the reduction in the available adsorption sites occupied by cross-linking agents [17]. Blending of CS with polyvinyl alcohol (PVA) as proposed was reported to give good mechanical strength and chemical resistivity, due to the occurrence of intra and intermolecular bonding [18,19]. CS/PVA composite has been used recently for the removal of heavy metal ions from aqueous solution [20–23].

In this study, we aim to study the effect of a tetraethoxysilane (TEOS) cross-linking agent on the adsorption properties of copper of a PVA blended CS. CS, CS/PVA, and CS/PVA/TEOS hydrogel beads were prepared and their Cu(II) adsorption performances

and mechanisms were studied and compared. The prepared materials were characterized by Fourier transform infrared (FTIR) spectroscopy and scanning electron microscopy (SEM). A series of batch adsorption experiments at different pH values, various amounts of adsorbent, initial copper concentrations, and contact time were conducted.

2. Experimental

2.1. Preparation of CS, CS/PVA, and cross-linked CS/PVA/TEOS beads

CS (DDA \geq 75%, molecular weight: \sim 150,000) flakes were prepared from locally available crab shells obtained from Karachi, Pakistan [24]. CS beads (\sim 1 mm diameter) were prepared according to published data [19,25]. Briefly, CS solution prepared in 0.5 M acetic acid was dropped in precipitation bath containing 25 wt.% NaOH solution with the help of a syringe.

In order to prepare composite CS/PVA beads, a 5 wt.% PVA (98.99%, average molecular weight: 146,000–186,000) solution, prepared in distilled water at 80–90 °C, was mixed with a 5 wt.% CS solution in 0.5 M acetic acid and stirred together for 1 h (60 and 40 wt.% of each component in CS/PVA composite whereas 57, 38, and 5 wt.% of each component in CS/PVA/TEOS beads, respectively). Moreover, for the preparation of cross-linked CS/PVA/TEOS beads, an appropriate amount of TEOS (98%, 208.33 g/mol) cross-linking agent solution (prepared in 99% ethanol) was added dropwise into the CS/PVA blend making (2 v/v%) ratio with the blend and it was stirred for 24 h.

The CS/PVA blend cross-linked or uncross-linked was also sprayed into a precipitation bath (25 wt.% NaOH) to convert the gel into some uniform and spherical beads using the same method previously described for CS beads.

All the wet beads were extensively rinsed with distilled water to remove any NaOH, filtered, and finally dried at room temperature. Fig. 1 shows the proposed structure of CS/PVA/TEOS composite and its interaction with Cu^{2+} ions.

2.2. Characterization of the beads

2.2.1. Solubility/chemical stability

The dissolution of CS/PVA and CS/PVA/TEOS beads was studied by adding 10 mg of beads in adjusted pH (from pH 2 to 9 by addition of 50 mL of 10^{-1} M hydrochloric acid or 10^{-1} M sodium hydroxide) distilled water solutions for a period of 24 h. To determine the beads solubility, total organic carbon

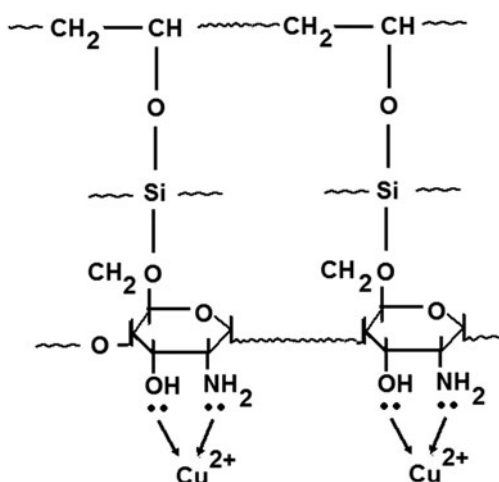


Fig. 1. Proposed cross-linked structure of CS/PVA/TEOS composite and its interaction with Cu^{2+} ions.

(OC), total carbon (TC), and total nitrogen (TN) contents were measured in the filtrated solutions using a TOC analyzer (TOC-V_{CSN} Shimadzu) coupled with a TN measuring unit.

The swelling ratio of the beads ($\frac{W_w - W_d}{W_d} \times 100$) was calculated from W_w and W_d , the weights (in g) of wet and dry beads, respectively. The beads were dried at 25°C for approximately 48 h to get constant weight.

2.2.2. FTIR analysis

The CS, CS/PVA, and cross-linked CS/PVA/TEOS beads were characterized by ATR-FTIR using a Thermo Scientific Nicolet iS10 spectrometer equipped with a germanium crystal. A DTGS KBr detector was used for detection and the incident angle of the beam was 45°. All the spectra were collected at spectral resolution of 4 cm^{-1} and average of 64 scans were reported.

2.2.3. SEM

Before SEM analysis, the beads were frozen in liquid nitrogen at 77 K and then cut from the middle with the help of a single-edged blade to get a cross-section. Samples were metallized with amorphous carbon to increase their conductivity and observed using a JEOL, JSM-6400 scanning microscope. Bruker silicon drift EDS detector coupled with the SEM was used to investigate the chemical nature of the samples.

2.2.4. BET surface area

The N_2 adsorption–desorption isotherms were measured using automatic sorptometer (ASAP 2000,

Micrometrics) at liquid nitrogen temperature (77 K). Prior to measurements the samples were degassed under vacuum (10^{-3} mbar) at 100°C for 12 h. The specific surface area was calculated using BET (Brunauer–Emmett–Teller) equation by assuming the area of a nitrogen molecule to be 0.162 nm^2 .

2.3. Adsorption studies

All chemical reagents were analytical grade, and distilled water (conductivity 1.5 $\mu\text{S}/\text{cm}$) was used for the preparation of the solutions. A stock solution of Cu(II) (1,000 mg/L) was prepared by dissolution of anhydrous CuSO_4 and was used to prepare solution of various concentrations by dilution (from 10 to 200 mg/L). Batch processes at ambient temperature (25°C) were carried out for adsorption experiments. The prepared beads were swelled in distilled water for 4 h before adsorption experiments.

For isothermal adsorption experiments, a known amount of water-swollen beads was placed in a flask containing 50 mL copper solution (10–200 mg/L range) and agitated in a shaker (Inova 44, incubator shaker series) at 250 rpm for 24 h. The concentration of the remaining adsorbate in the filtrated solution was determined using atomic absorption spectroscopy (Shimadzu atomic adsorption/flame emission AA-660), and the adsorbed amount of copper ions (Q) was calculated from the following equation: $Q = (C_0 - C_1) V_s / 1000 / W_b$, where C_0 and C_1 are the initial and final concentrations (mg/L) before and after adsorption in solution, V_s is the volume of experimental solution (L), and W_b is the weight (g) of the beads.

For kinetics studies, adsorption experiments at 25°C were carried out by varying contact time (10 min to 24 h at initial concentration of 10 mg/L). The effect of the adsorbent dose was studied by varying the amount of adsorbent (5–250 mg) at an initial concentration of $C_0 = 10$ mg/L and a contact time of 16 h. A series of experiments were carried out by taking fixed amount of adsorbent (10 mg) and initial concentration of the adsorbate solution (10 mg/L) for different pH values (from 3 to 7) at room temperature (25°C). Adsorption isotherms were recorded at three temperatures (287.5, 298, and 313 K) in order to determine the thermodynamic parameters of the adsorption.

3. Results and discussion

3.1. Solubility/chemical stability of the beads

The cross-linked CS/PVA/TEOS beads were visually insoluble in distilled water, as well as in weakly acidic ($\text{pH} \geq 3$), and alkaline media ($\text{pH} \geq 9$). They

seemed to be partially soluble in acidic aqueous solutions of pH ~2. The presence of primary amino groups in raw CS confirmed by IR spectra gives high hydrophilic characteristics, so it can easily be dissolved in acidic media (i.e. in acetic or hydrochloric acid). The solubilities of CS, CS/PVA, and cross-linked CS/PVA/TEOS beads were measured at various pH on the basis of TC, TN, and OC. Table 1 demonstrates the soluble nature of CS at pH lower or equal to 4, while the CS/PVA composites (cross-linked or uncross-linked) start to dissolve at pH lower than 4. Cross-linking is quite essential to reinforce the chemical stability of the polymer like CS in acidic media.

The characterization of swelling behavior in distilled water depicted that cross-linked CS/PVA/TEOS beads have higher swelling capacities than other CS beads. A swelling ratio of 115% was measured for CS/PVA/TEOS beads compared with 70% for CS beads. The swelling of the cross-linked CS/PVA/TEOS beads was found to be reduced by a factor of two after copper loading, reaching 60%, which suggested a removal of adsorbed water from the adsorption sites.

3.2. FTIR analysis

IR spectrum of CS (Fig. 2(a)) displays peaks at 1,658, 1,580, and 1,420 cm^{-1} , which are the characteristic absorption bands for amide-I (the carbonyl stretching, $\nu\text{C}=\text{O}$), amide-II (the NH bending, δNH), and $-\text{CH}_2$ bending, respectively, belonging to CS molecule [26]. Absorption bands at 1,150 cm^{-1} is for antisymmetric stretching of C–O–C bridge, while 1,070, 1,030, and 936 cm^{-1} are for C–O vibration stretching, and all these peaks may explain saccharide structural presence in CS. Strong broad peak at about 3,400 cm^{-1} is due to OH stretching vibrations; superimposed bands at 3,300–3,500 cm^{-1} are due to N–H symmetrical vibration stretching of N–H group in CS. Meanwhile, in PVA spectrum (Fig. 2(b)) this influential peak attributed to O–H stretching of alcohol group is also present between

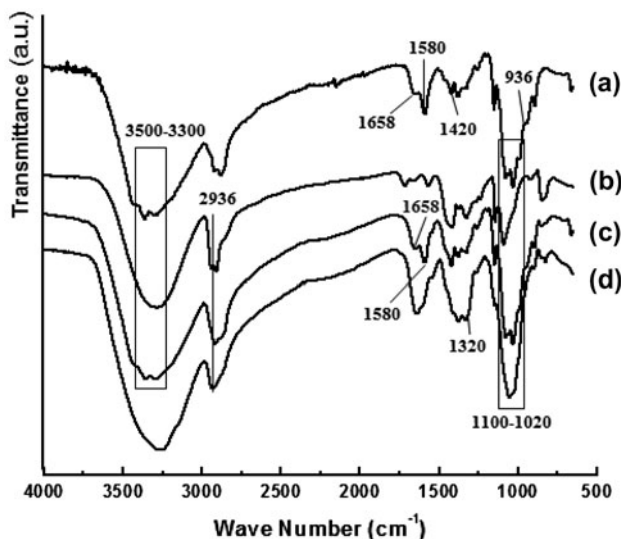


Fig. 2. FTIR spectra of (a) pure CS, (b) PVA, (c) cross-linked CS/PVA/TEOS beads, and (d) Cu-adsorbed cross-linked CS/PVA/TEOS beads.

3,200 and 3,550 cm^{-1} . Two other significant peaks at 2,936 and 835 cm^{-1} are designated to CH and CH_2 asymmetric stretching vibration and C–H rocking mode for PVA respectively [27]. A slight increase in the intensity of peaks between 1,020 and 1,100 cm^{-1} of the cross-linked CS/PVA/TEOS hydrogel beads (Fig. 2(c)), confirming the presence of Si–O–Si and also Si–O–C linkage and support the cross-linking of TEOS between CS and PVA. After copper adsorption (Fig. 2(d)), the peaks at 1,658, 1,580, and 3,360 cm^{-1} disappear and the intensities of the peaks at 1,070–1,030 cm^{-1} significantly decrease indicating that Cu^{2+} ions are mainly engaged with $-\text{NH}_2$ group as adsorption sites. After Cu adsorption, significant change in the FTIR spectra are also found at 1,320 cm^{-1} which can be assigned to C–N stretching vibration of CS molecules. The increase in intensity of this peak after adsorption was previously attributed to the formation of N–Cu–O groups [28].

Table 1

Total carbon (TC), total nitrogen (TN), and total organic carbon (OC) concentration (in ppm) of a dispersion of CS, CS/PVA, and cross-linked CS/PVA/TEOS beads (10 mg in 50 mL)

Beads	pH 2			pH 4			pH 6			pH 7			pH 9		
	TC	TN	OC	TC	TN	OC	TC	TN	OC	TC	TN	OC	TC	TN	OC
CS	83.3	13.2	74.8	62.4	0.6	25.7	41.8	0.2	7.1	0.9	0	0	0	0	0
CS/PVA	71.5	8.8	52.6	1.3	0.1	0	1.8	0	0	2.2	0.1	0	2.7	0	0
CS/PVA/TEOS	61.7	9.4	65.6	0.8	0	0	0.3	0	0	1.1	0	0	1.8	0	0

3.3. Porosity and morphology

The values of BET specific surface areas measured by nitrogen adsorption were very low and quite similar for all the studied CS-based materials (in the range 0.2–0.5 m²/g). The values of pore volumes were found

negligible, showing that the beads were neither microporous nor mesoporous materials.

SEM micrographs of CS/PVA and cross-linked CS/PVA/TEOS beads are shown in Fig. 3. SEM images of the surfaces of the beads (Fig. 3(a)–(d))

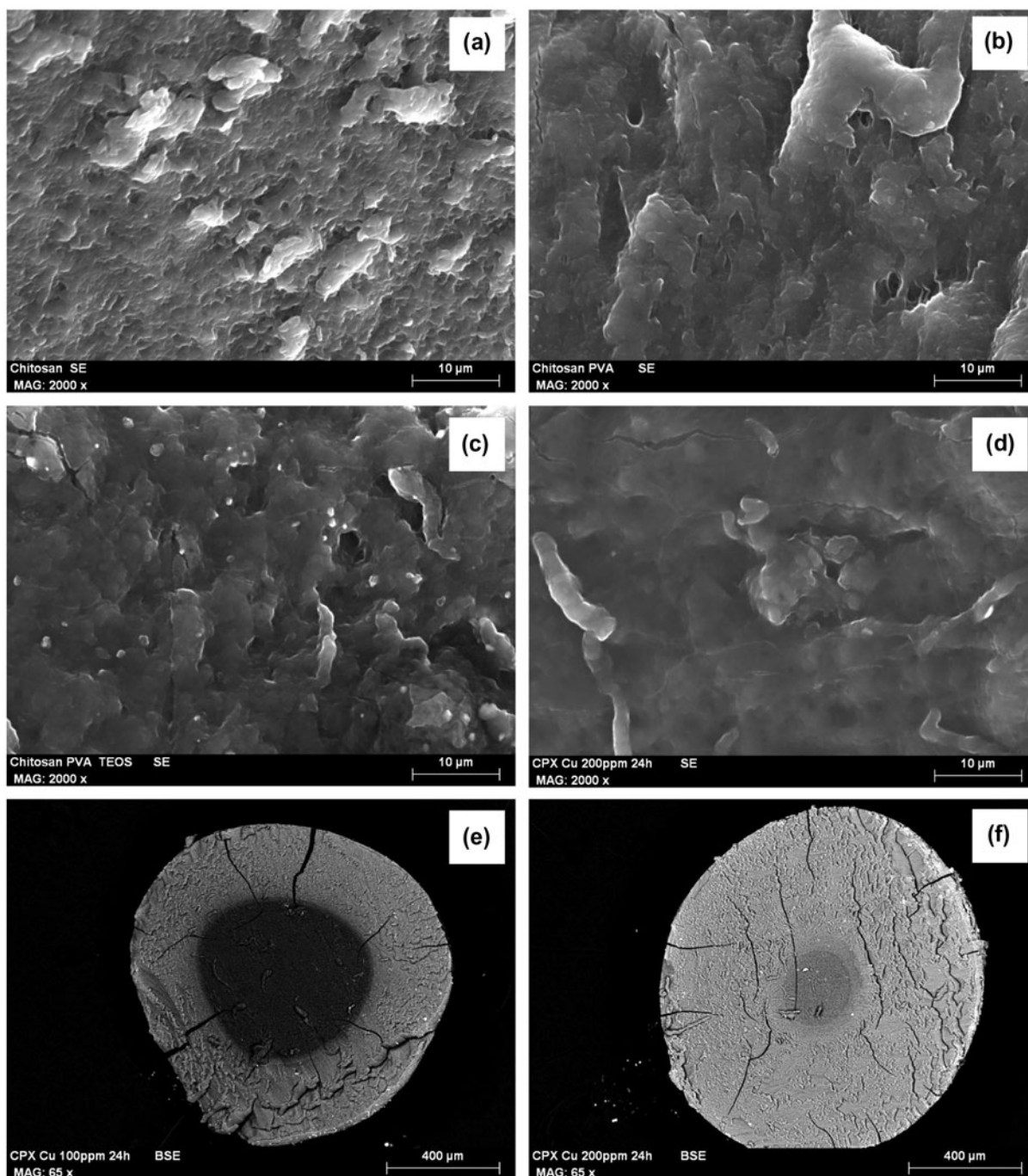


Fig. 3. SEM images of surfaces of CS beads (a), CS/PVA beads (b), CS/PVA/TEOS beads before adsorption (c), after Cu²⁺ adsorption for $Q_{\text{ads}} = 131$ mg/g (d), and of cross sections of CS/PVA/TEOS beads after adsorption of Cu²⁺ for $Q_{\text{ads}} = 75$ mg/g and $Q_{\text{ads}} = 131$ mg/g respectively (e and f).

show the presence of macropores in CS, CS/PVA, and cross-linked CS/PVA/TEOS beads (pore size $\sim 2\mu\text{m}$). The surface of CS beads is the roughest (Fig. 3(a)) and it decreases with the successive chemical treatments with PVA and TEOS, highlighting a modification of the mechanical properties as expected.

The cross-sections of cross-linked CS/PVA/TEOS beads after 24 h of Cu loading, observed in the backscattering electron mode, display the adsorption front of Cu^{2+} cations (Fig. 3(e) and (f)). For an uptake of 75 mg/g (obtained by dispersing 10 mg of CS/PVA/TEOS beads in 50 mL of 100 ppm Cu^{2+} solution), about $15\text{ vol.}\%$ of the bead was loaded with copper, as confirmed by the presence of a lighter outer ring in Fig. 3(e). EDX analyses confirmed the presence of only copper within this ring. Despite the apparently attained complete saturation after 24 h of contact time and an uptake of 131 mg/g (obtained by dispersing 10 mg of CS/PVA/TEOS beads in 50 mL of 200 ppm Cu^{2+} solution), the central spherical domain was not completely saturated by the metal cation (Fig. 3(f)). The diffusion profile of copper inside this sample, evidenced by EDX analyses, shows a lower copper content in the center of the bead compared with the external surface (Fig. 4). The copper adsorption decreases slightly from the external to the internal surface and

is minimum in a sphere of $200\mu\text{m}$ diameter located in the center of the bead (Fig. 4). In fact, the SEM image (Fig. 3(f)) indicates that only $0.8\text{ vol.}\%$ of the bead was unloaded with copper, so that the saturation was almost attained. This demonstrates that the adsorption proceeds through a diffusion of the metallic cation from the external surface toward the bulk of the beads, and that the theoretical saturation might be attained for contact time higher than 24 h.

3.4. Effect of pH on copper adsorption

The pH has a key role in the adsorption phenomena and strongly affects the adsorption capacity of the metal ions. According to Pourbaix diagram for copper, pH values lower than 7 is recommended in order to avoid precipitation of copper as hydroxide at higher pH [29]. The adsorption uptake of copper against pH for 10 mg of adsorbent can be seen in Fig. 5, showing that maximum loading capacity is at pH 6. At low pH, the $-\text{NH}_2$ amino groups of CS are protonated as $-\text{NH}_3^+$ repels other positive ion (i.e. Cu^{2+}) yielding to low adsorption uptake. In order to achieve the maximum uptake and also avoid precipitation, pH for copper adsorption studies was compromised at 6.

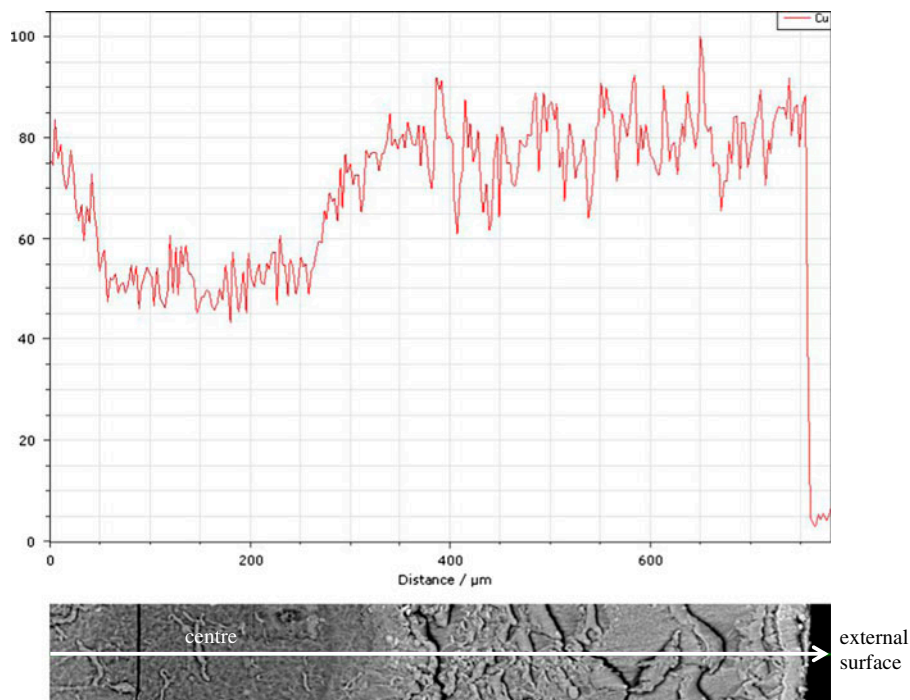


Fig. 4. EDX diffusion profile of copper inside a CS/PVA/TEOS bead ($Q_{\text{ads}} = 131\text{ mg/g}$).

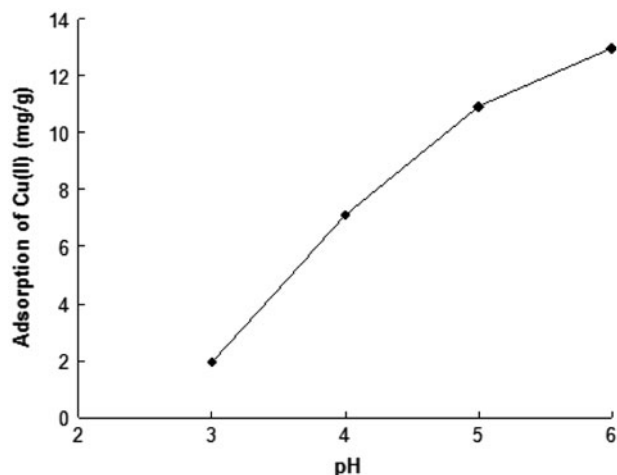


Fig. 5. Effect of pH on Cu^{2+} adsorption for cross-linked CS/PVA/TEOS beads ($T = 25^\circ\text{C}$, $C_0 = 10 \text{ mg/L}$, $V = 50 \text{ mL}$, agitation speed = 250 rpm, adsorbent dose = 10 mg).

3.5. Effect of adsorbent dose

The effect of adsorbent dose on the adsorption of copper is studied and results are shown in Fig. 6. The amount of adsorbent varied from 5 to 250 mg. This figure shows that as the amount of adsorbent increased, the percentage of copper ions removed from the solution was enhanced due to the increasing number of sites within the adsorbent. At a particular amount (5 g/L), no further removal of metal ions took place and this behavior is exhibited for almost all the adsorbents [30]. Fig. 6 also exhibits that as the amount of adsorbent increased the uptake (mg/g) of the adsorbent was decreased. This is due to two main reasons (i) with the increase in the adsorbent amount

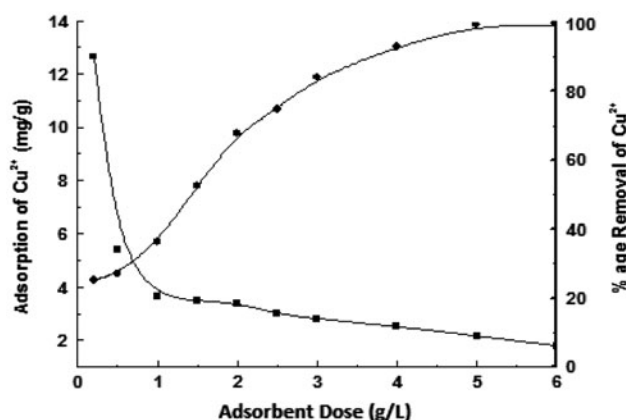


Fig. 6. Effect of adsorbent dose on Cu^{2+} adsorption ($T = 25^\circ\text{C}$, $C_0 = 10 \text{ mg/L}$, agitation speed = 250 rpm, 24 h and pH 6).

there is increase in the unsaturation sites of the adsorbent and (ii) particulate interaction like aggregation resulting in high adsorbent amount which was observed visually in this particular case. Such aggregation forefronts to a decrease in total surface area of the adsorbent and also increase the diffusional path length.

3.6. Adsorption kinetics

Adsorption kinetics is quite necessary to determine the time required for the copper ions uptake on the adsorbent and the rate limiting step for transport mechanism. The adsorption kinetics behavior of metal ions was analyzed with regards to some typical theoretical models and that information is useful in the modeling and process design [31,32].

The adsorption phenomena for the uptake of metal ions onto the surface of the hydrogel beads can be proceeded on the following two hypothesis: (i) the transport of the metal ions from the bulk solution to the surfaces of adsorbent (beads) and (ii) the attachment of metal ions to the active adsorption sites of the hydrogel beads [33]. To examine the adsorption mechanisms: pseudo-first-order, pseudo-second-order, and interparticle diffusion models were applied (at $C_0 = 10 \text{ ppm}$, adsorbent = 10 mg, pH 6, Agitation speed = 250 rpm and $T = 25^\circ\text{C}$). The model equations can be expressed as in Eqs. (1)–(3).

$$\ln(Q_e - Q_t) = \ln Q_e - k_1 t \quad (1)$$

$$\frac{t}{Q_t} = \frac{1}{k_2 Q_e^2} + \frac{t}{Q_e} \quad (2)$$

$$Q_t = k_3 t^{0.5} \quad (3)$$

where Q_e and Q_t (mg/g) are the copper ion adsorption amounts onto beads at equilibrium and time " t " and k_1 , k_2 , and k_3 are the rate constants of the pseudo-first-order, pseudo-second-order and diffusion models, respectively.

The curve fitting of all three models to the experimental data (Fig. 7) and their parameters are tabulated in Table 2. For adsorption onto cross-linked CS/PVA/TEOS beads, the correlation coefficients (R^2) for all models were very close (about 0.97–0.98), indicating that all models can explain adsorption kinetics of copper ions onto beads.

Fig. 7(a) and (b) show the matching of both the pseudo-first-order and pseudo-second-order models to the experimental data. In Fig. 7(c), only one type of

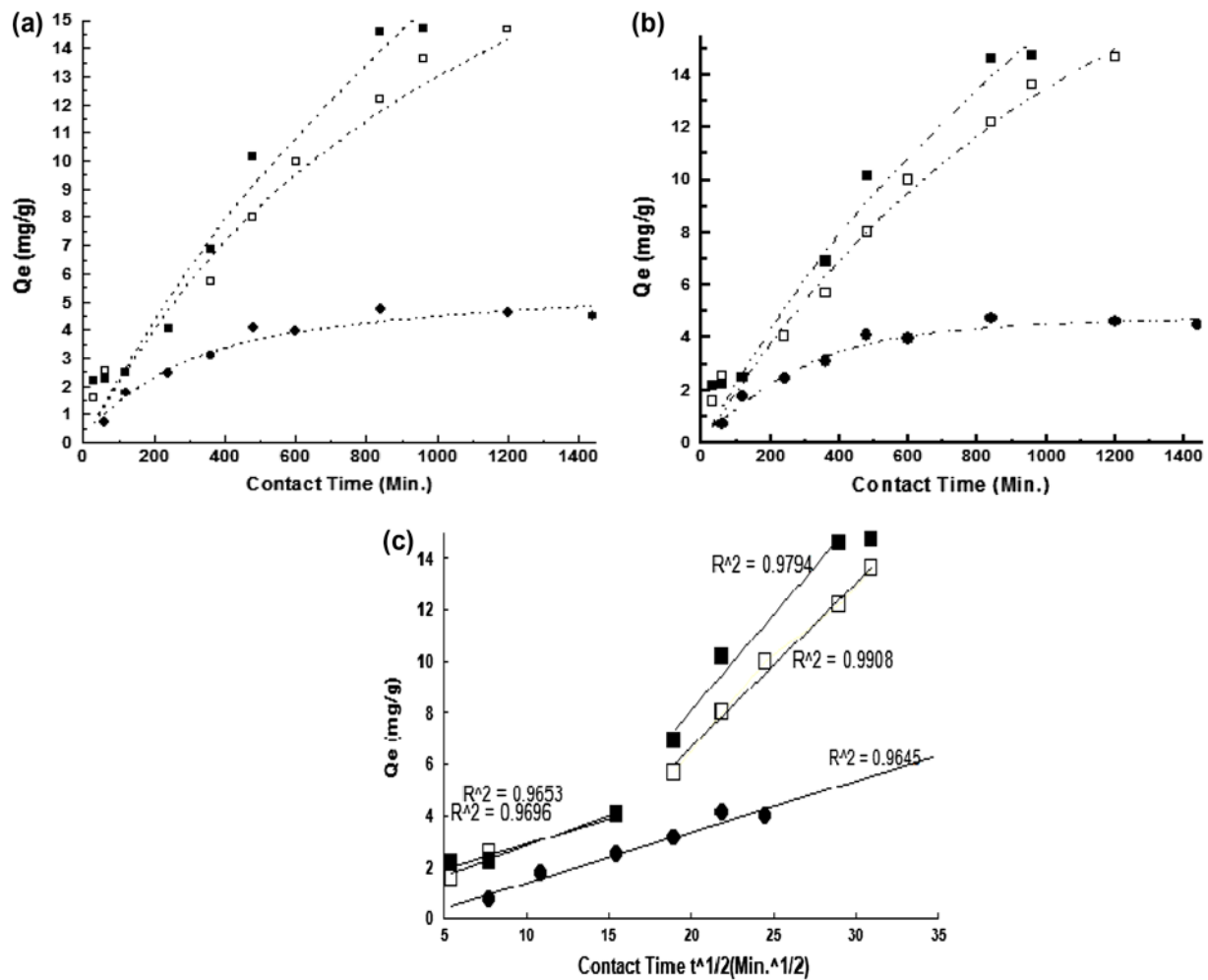


Fig. 7. Kinetics fits of (a) pseudo-first-order model, (b) pseudo-second-order model and (c) linear form of inter-particle diffusion model, for CS (full circle), CS/PVA (empty square), and cross-linked CS/PVA/TEOS (full square) beads.

Table 2

Kinetic parameters for adsorption of Cu^{2+} onto cross-linked CS/PVA/TEOS beads ($T = 25^\circ\text{C}$, $C_0 = 10 \text{ mg/L}$, agitation speed = 250 rpm, adsorbent dose = 10 mg, and pH 6)

Constants	k_1 1st order min^{-1}	k_2 2nd order $\text{g}/(\text{mg min})$	k_3 Diffusion ($t < 225 \text{ min}$) $\text{mg}/(\text{g min}^{1/2})$	k_3 Diffusion ($t > 225 \text{ min}$) $\text{mg}/(\text{g min}^{1/2})$
Values	9.1×10^{-4}	1.2×10^{-5}	19.64×10^{-2}	74.52×10^{-2}
R^2	0.9670	0.9670	0.9652	0.9794
RMSE	0.977	0.984	–	–

diffusion was observed for pure CS beads corresponding to one straight line. By contrast, two diffusion rates were observed in PVA blended CS beads corresponding to two different linear representations of uptake vs. $t^{1/2}$ for two successive time periods. This can be explained by the presence of two different sites for

adsorption of copper. As the first time period diffusion ($< 225 \text{ min}$) are similar for CS, CS/PVA, and cross-linked CS/PVA/TEOS, it suggests the presence of specific sites from pure CS in the composites. The other adsorption sites might be specific of the composite and originating from PVA or cross-linked PVA. Moreover,

first adsorption is slower and it might occur on CS site (for $t < 15^2 = 225$ min) and the second quicker adsorption might be on specific PVA site (from 225 to 900 min). This might also indicate the heterogeneous nature of the adsorbent made of small domain of PVA covered by CS. As a conclusion, the interparticle diffusion model appears to be more appropriate to explain the mass transport control in the copper adsorption process as the SEM images (Fig. 3(e)) have also shown its diffusion limitation in the beads.

3.7. Equilibrium isotherms

The adsorption equilibrium capacity of the prepared materials was also compared with some other CS-based adsorbents published in the recent past and tabulated in Table 3. In all previous studies, the Langmuir and Freundlich isotherm models constants have been calculated for the adsorption process of Cu^{2+} . For copper adsorption, the maximum adsorption uptake obtained for TEOS cross-linked CS/PVA beads (220 mg/g) at pH 6 and the $C_o = 125$ mg/L is quite in agreement with the highest adsorption uptakes found for CS-based materials. Moreover, the cross-linking of CS/PVA with TEOS not only improved the uptake of Cu^{2+} but it also increased its chemical and mechanical stability, especially, in acidic media.

The Langmuir (Eq. (4)) and Freundlich (Eq. (5)) isotherm models (Fig. 8) are well reproducing the adsorption uptake of Cu^{2+} on the different adsorbents:

$$Q_e = \frac{Q_m K_L C_e}{1 + K_L C_e} \quad (4)$$

$$Q_e = K_F C_e^{1/n} \quad (5)$$

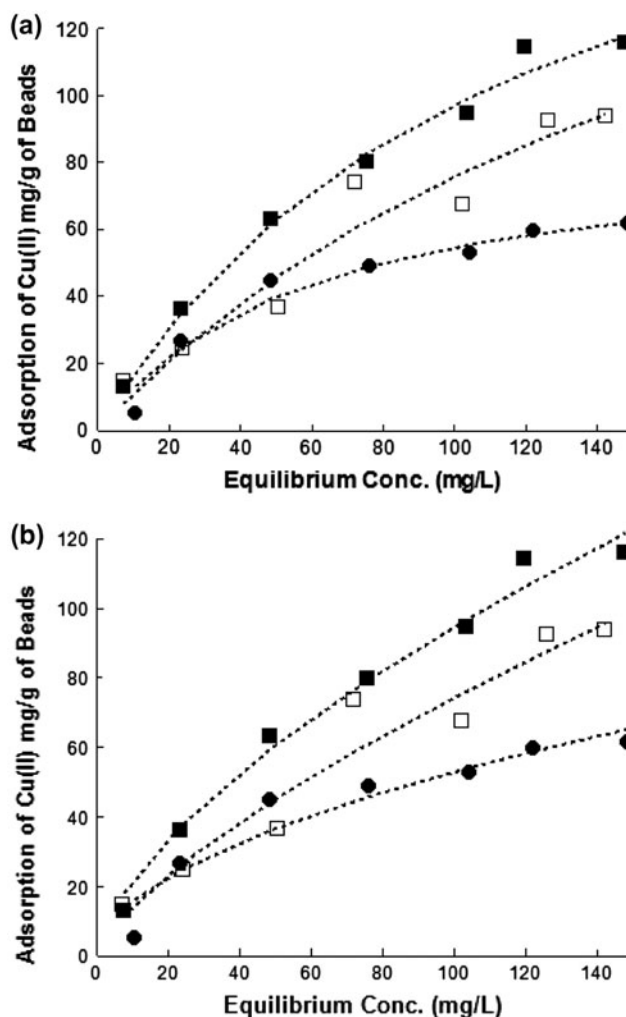


Fig. 8. Experimental isotherms at 298 K for CS (full circle), CS/PVA (empty square), and cross-linked CS/PVA/TEOS (full square) beads fitted with Langmuir (a) and Freundlich (b) models (dashed lines).

Table 3
Adsorption capacity of different CS based adsorbents for Cu^{2+}

Adsorbent	Adsorption capacity (mg/g)	Reference
Gel/CS composite	870.0	Gandhi and Meenakshi [34]
CS-g-PAA	262.2	Wang et al. [35]
CS/PVA/TEOS beads	224.6 (Q_m value)	Present study
CS/PVA beads	186.6 (Q_m value)	Present study
CS	86.3 (Q_m value)	Present study
Surfactant acidified CS beads	221.5	Sarkar and Majumdar [36]
CS/ZSM	137.9	Li and Huang [37]
CS-ECH-TPP	130.72	Laus and Fávere [38]
CS-coated PVC beads	87.9	Popuri et al. [39]
CS/PVA	47.85	Ngah et al. [19]
CS	33.44	Ngah et al. [19]

Table 4

Equilibrium isotherm parameters for adsorption of Cu^{2+} onto cross-linked CS/PVA/TEOS beads (agitation speed = 250 rpm, adsorbent dose = 10 mg and pH 6)

Temperature (K)	Langmuir model			Freundlich model		
	Q_m (mg/g)	K_L (L/g)	R^2	n	K_F	R^2
287.5	110.5	8.5	0.958	1.66	3.07	0.934
298.0	210.8	8.5	0.988	1.56	4.98	0.981
313.0	224.6	10.2	0.987	1.65	6.71	0.982

Table 5

Thermodynamic parameters for adsorption of Cu^{2+} onto cross-linked CS/PVA/TEOS beads

Model	ΔG° (kJ/mol)	ΔH° (kJ/mol)	ΔS° (J/mol K)
Arrhenius law	–	7.5	–
Gibbs law ($Q_e = 10$ mg/L)	–0.8	26.5	91.7
Gibbs law ($Q_e = 50$ mg/L)	–0.03	34.9	117.3

where C_e is the equilibrium concentration (mg/L), Q_e and Q_m are the adsorption at equilibrium and maximum adsorption capacity (mg/g), respectively. K_L , K_F , and n are the adsorption equilibrium constants for Langmuir and Freundlich models, respectively. The n value in the Freundlich model is indicative of adsorption intensity and known as the heterogeneity factor (range 0–1).

Langmuir model supposes a homogeneous adsorption on similar sites within the adsorbent forming a saturated monolayer. On the other hand, Freundlich model is an empirical equation based on the assumption of adsorption on heterogeneous surfaces and can be applied for multi-layer adsorption. The equilibrium isotherm constants at three temperatures (Table 4) for cross-linked CS/PVA/TEOS beads show that Langmuir model agrees better with the experimental data than Freundlich one.

3.8. Thermodynamics

The standard enthalpy variation (ΔH°) can be calculated from the Arrhenius law applied to the kinetics rate constants from which K_L Langmuir constant is derived, as in Eq. (6): $K_L = K_0 \exp(-\Delta H^\circ/RT)$, where R and T are the universal gas constant (kJ/mol K) and the absolute temperature (K), respectively.

The data computed by the Langmuir simulations were used to determine the Gibbs energy from the equation Eq. (7): $\ln(C_a/C_e) = -\Delta G^\circ/RT$, where T is the temperature of the solution (K) and C_a is the amount of copper adsorbed from solution at equilibrium (mg/L). The equilibrium constant for the adsorption

equal to $K_d = C_a/C_e$ was calculated by using the adsorption equilibrium using the Langmuir law (Eq. (4)). Using the equation $\Delta G^\circ = \Delta H^\circ - T\Delta S^\circ$, the isotheric enthalpies and entropies of adsorption were determined graphically from the linear plot of $\ln(K_d)$ vs. $1/T$. The isosteric enthalpies (ΔH°) were calculated from the slope of this curve and the entropies of adsorption (ΔS°) were calculated from the y intercept.

All the thermodynamic constants for the adsorption of copper ions onto cross-linked CS/PVA/TEOS beads are compiled in Table 5. The adsorption of copper cation on the CS was found to be endothermic using either Arrhenius law or Gibbs law, possibly because its stable bond with solvent as an aqua $[\text{Cu}(\text{H}_2\text{O})_6]^{2+}$ complex needs to be broken to form a new complex with CS, and it costs energy. The endothermic nature of this adsorption increases together with the concentration because the adsorption sites are energetically heterogeneous, so that the less energetic sites are first occupied at the lowest concentrations of copper ions.

The slightly negative ΔG° values can be explained by the strong endothermic nature of copper adsorption (in the range 20–75 kJ/mol) indicating a chemisorption process. This chemisorption might be due to the chelation of copper with NH_2 and OH groups of CS and PVA. Moreover, the removal of adsorbed water from cross-linked CS/PVA/TEOS beads after copper loading (measured by weight loss at 55 wt.%) confirms the positive value of ΔS° (increase of disorder). This also suggests that the chemisorption of Cu^{2+} is entropy driven, because metal cations occupy the site of physisorbed water molecules which are removed after adsorption.

4. Conclusion

In present study, beads of CS containing PVA were successfully cross-linked with TEOS. These chemically and mechanically stable beads were used as adsorbent between pH range of 3–14 and harsh conditions (elevated solution temperature) for the removal of Cu^{2+} ions from wastewater. The adsorption kinetics was controlled by diffusion from the external surface of the beads to the bulk. The adsorption of Cu^{2+} ions from aqueous solution on cross-linked CS/PVA/TEOS is very much influenced by initial pH of solution, contact time, initial concentration of solution, amount of adsorbent, and temperature. The equilibrium adsorption data were satisfactorily fitted to Langmuir or Freundlich isotherm models. According to Langmuir model, maximum adsorption capacity of Cu^{2+} ions is 224.6 mg/g at 313 K. The adsorption mechanism implies the break of the water–copper bonds in the aqua complex yielding an endothermic process. The chelation of the copper cations onto the –OH or –NH sites of the cross-linked CS/PVA/TEOS materials induced the dehydration of the beads due to the release of water from the Cu^{2+} adsorption sites. In prospects, the amount of cross-linker could be optimized to avoid dissolution at lower pH (pH 1) without hindering adsorption, and the bead size could be reduced to accelerate the kinetics.

Acknowledgments

The authors and particularly Muhammad Arif Kamal acknowledge the funding from the French Embassy in Islamabad and the support of the Higher Education Commission of Pakistan for a six months sandwich fellowship in University of Savoie (France).

References

- [1] M. Monier, Adsorption of Hg^{2+} , Cu^{2+} and Zn^{2+} ions from aqueous solution using formaldehyde cross-linked modified chitosan–thioglyceraldehyde Schiff's base, *Int. J. Biol. Macromol.* 50 (2012) 773–781.
- [2] J.H. Chen, H. Lin, Z.H. Luo, Y.S. He, G.P. Li, Cu(II)-imprinted porous film adsorbent Cu-PVQ-SA has high uptake capacity for removal of Cu(II) ions from aqueous solution, *Desalination* 277 (2011) 265–273.
- [3] N.D. Tumin, A.L. Chuah, Z. Zawani, S.A. Radish, Adsorption of copper from aqueous solution by Elais Guineensis Kernel activated carbon, *J. Eng. Sci. Technol.* 3 (2008) 180–189.
- [4] M. Teker, M. Imamoglu, O. Saltabas, Adsorption of copper and cadmium ions by activated carbon from rice hulls, *Turk. J. Chem.* 23 (1999) 185–191.
- [5] A.T. Paulino, F.A.S. Minasse, M.R. Guilherme, A.V. Reis, E.C. Muniz, J. Nozaki, Novel adsorbent based on silkworm chrysalides for removal of heavy metals from wastewaters, *J. Colloid Interface Sci.* 301 (2006) 479–487.
- [6] J. Wang, L. Ding, J. Wei, F. Liu, Adsorption of copper ions by ion-imprinted simultaneous interpenetrating network hydrogel: Thermodynamics, morphology and mechanism, *Appl. Surf. Sci.* 305 (2014) 412–418.
- [7] J. Wang, X. Li, Ion-imprinted poly(2-acrylamido-2-methyl-1-propansulfonic acid)/modified silica composite hydrogel for selective and enhanced adsorption of Pb(II) ions, *Desalin. Water Treat.* 52 (2014) 274–282.
- [8] Z.R. Liu, S. Zhou, Adsorption of copper and nickel on Na-bentonite, *Process Saf. Environ.* 88 (2010) 62–66.
- [9] M. Kumar, B.P. Tripathi, V.K. Shahi, Crosslinked chitosan/polyvinyl alcohol blend beads for removal and recovery of Cd(II) from wastewater, *J. Hazard. Mater.* 172 (2009) 1041–1048.
- [10] N. Karapinar, R. Donat, Adsorption behaviour of Cu^{2+} and Cd^{2+} onto natural bentonite, *Desalination* 249 (2009) 123–129.
- [11] E.C. Lima, B. Royer, J.C.P. Vaghetti, J.L. Brasil, N.M. Simon, A.A. Dos Santos Jr., F.A. Pavan, S.L.P. Dias, E.V. Benvenuti, E.A. Da Silva, Adsorption of Cu(II) on Araucaria angustifolia wastes: Determination of the optimal conditions by statistic design of experiments, *J. Hazard. Mater.* 140 (2007) 211–220.
- [12] A.H. Chen, S.C. Liu, C.Y. Chen, C.Y. Chen, Comparative adsorption of Cu(II), Zn(II), and Pb(II) ions in aqueous solution on the crosslinked chitosan with epichlorohydrin, *J. Hazard. Mater.* 154 (2008) 184–191.
- [13] J.H. Hamman, Chitosan based polyelectrolyte complexes as potential carrier materials in drug delivery systems, *Mar. Drugs* 8 (2010) 1305–1322.
- [14] L. Zhou, J. Liu, Z. Liu, Adsorption of platinum(IV) and palladium(II) from aqueous solution by thiourea-modified chitosan microspheres, *J. Hazard. Mater.* 172 (2009) 439–446.
- [15] A. Kamari, W.S.W. Ngah, L.K. Liew, Chitosan and chemically modified chitosan beads for acid dyes sorption, *J. Environ. Sci.* 21 (2009) 296–302.
- [16] C. Jeon, W.H. Höll, Chemical modification of chitosan and equilibrium study for mercury ion removal, *Water Res.* 37 (2003) 4770–4780.
- [17] X.J. Hu, J.S. Wang, Y.G. Liu, X. Li, G.M. Zeng, Z.L. Bao, X.X. Zeng, A.W. Chen, F. Long, Adsorption of chromium (VI) by ethylenediamine-modified cross-linked magnetic chitosan resin: isotherms, kinetics and thermodynamics, *J. Hazard. Mater.* 185 (2011) 306–314.
- [18] J.L. Jin, R. Bai, Mechanisms of lead adsorption on Chitosan/PVA hydrogel beads, *Langmuir* 18 (2002) 9765–9770.
- [19] W.S.W. Ngah, A. Kamari, Y.J. Koay, Equilibrium and kinetics studies of adsorption of copper (II) on chitosan and chitosan/PVA beads, *Int. J. Biol. Macromol.* 34 (2004) 155–161.
- [20] Q.B. Wei, Y.L. Luo, L.J. Gao, Q. Wang, D.J. Wang, Synthesis, characterization and swelling kinetics of thermoresponsive PAM-g-PVA/PVP semi-IPN hydrogels, *Polym. Sci. Ser. A* 53 (2011) 707–714.
- [21] X.Y. Wu, S.W. Huang, J.T. Zhang, R.X. Zhuo, Preparation and characterization of novel physically cross-linked hydrogels composed of poly(vinyl alcohol) and amine-terminated polyamidoamine dendrimer, *Macromol. Biosci.* 4 (2004) 71–75.

- [22] S.J. Kim, C.K. Lee, S.I. Kim, Characterization of the water state of hyaluronic acid and poly(vinyl alcohol) interpenetrating polymer networks, *J. Appl. Polym. Sci.* 92 (2004) 1467–1472.
- [23] X. Li, Y. Li, Z. Ye, Preparation of macroporous bead adsorbents based on poly(vinyl alcohol)/chitosan and their adsorption properties for heavy metals from aqueous solution, *Chem. Eng. J.* 178 (2011) 60–68.
- [24] A.G. Hadi, Adsorption of Cd(II) ions by synthesize chitosan from fish shells, *Br. J. Sci.* 5 (2012) 33–38.
- [25] M. Beigi, S.A. Babapoor, V. Maghsoodi, S.M. Mousavi, N. Rajabi, Batch equilibrium and kinetics studies of Cd (II) ion removal from aqueous solution using porous chitosan hydrogel beads, *Iran J. Chem. Eng.* 28 (2009) 81–89.
- [26] Y. Shigemasa, H. Matsuura, H. Sashiwa, H. Saimoto, Evaluation of different absorbance ratios from infrared spectroscopy for analyzing the degree of deacetylation in chitin, *Int. J. Biol. Macromol.* 18 (1996) 237–242.
- [27] H.A. Shawky, Synthesis of ion-imprinting chitosan/PVA crosslinked membrane for selective removal of Ag(I), *J. Appl. Polym. Sci.* 114 (2009) 2608–2615.
- [28] Z. Cheng, X. Liu, M. Han, W. Ma, Adsorption kinetic character of copper ions onto a modified chitosan transparent thin membrane from aqueous solution, *J. Hazard. Mater.* 182 (2010) 408–415.
- [29] M. Pourbaix, Atlas of Electrochemical Equilibria in Aqueous Solutions, National Association of Corrosion Engineers, Houston, TX, 1974.
- [30] W.S.W. Ngah, S. Fatinathan, Adsorption of Cu(II) ions in aqueous solution using chitosan beads, chitosan–GLA beads and chitosan–alginate beads, *Chem. Eng. J.* 143 (2008) 62–72.
- [31] J. Dai, H. Yang, H. Yan, Y. Shangguan, Q. Zheng, R. Cheng, Phosphate adsorption from aqueous solutions by disused adsorbents: Chitosan hydrogel beads after the removal of copper(II), *Chem. Eng. J.* 166 (2011) 970–977.
- [32] Y.A. Aydin, N.D. Aksoy, Adsorption of chromium on chitosan: Optimization, kinetics and thermodynamics, *Chem. Eng. J.* 151 (2009) 188–194.
- [33] J.J. Wang, F. Liu, Enhanced adsorption of heavy metal ions onto simultaneous interpenetrating polymer network hydrogels synthesized by UV irradiation, *Polym. Bull.* 70 (2013) 1415–1430.
- [34] M.R. Gandhi, S. Meenakshi, Preparation and characterization of silica gel/chitosan composite for the removal of Cu(II) and Pb(II), *Int. J. Biol. Macromol.* 50 (2012) 650–657.
- [35] X. Wang, Y. Zheng, A. Wang, Fast removal of copper ions from aqueous solution by chitosan-g-poly(acrylic acid)/attapulgitite composites, *J. Hazard. Mater.* 168 (2009) 970–977.
- [36] M. Sarkar, P. Majumdar, Application of response surface methodology for optimization of heavy metal bio-sorption using surfactant modified chitosan bead, *Chem. Eng. J.* 175 (2011) 376–387.
- [37] H. Li, D. Huang, Microwave preparation and copper ions adsorption properties of crosslinked chitosan/ZSM molecular sieve composites, *J. Appl. Polym. Sci.* 129 (2013) 86–93.
- [38] R. Laus, V.T. Fávere, Competitive adsorption of Cu(II) and Cd(II) ions by chitosan crosslinked with epichlorohydrin–triphosphate, *Bioresour. Technol.* 102 (2011) 8769–8776.
- [39] S.R. Popuri, Y. Vijaya, V.M. Boddu, K. Abburi, Adsorptive removal of copper and nickel ions from water using chitosan coated PVC beads, *Bioresour. Technol.* 100 (2009) 194–199.